Journal of the Korean Electrochemical Society
Vol. 3, No. 2, 2000, 76-80

Electrochemical Oxidation of Ethanol at RuO_2-Modified Nickel Electrode in Alkaline Media Studied by Electrochemical Impedance Spectroscopy

Jae-Woo Kim and Su-Moon Park†

School of Environmental Engineering and Department of Chemistry, Pohang University of Science and Technology, Pohang 790-784, Korea

(Received October 1, 1999 : Accepted March 2, 2000)

Abstract

Electrochemical oxidation of ethanol has been studied at nickel and RuO_2-modified nickel electrodes in 1 M KOH using electrochemical impedance spectroscopy. Equivalent circuits have been worked out from simulation of impedance data to model oxidation of ethanol as well as the passivation of the electrode. The charge-transfer resistances for oxidation of these electrodes became smaller in the presence of ethanol than in its absence. The nickel substrate facilitated ethanol oxidation at RuO_2-modified nickel electrodes. We also describe the performance of nanosized electrocatalysts of the same composition in comparison to those of the bulk electrodes. The nanosized electrodes were obtained by electrodepositing the alloy from complexed form of these metal ions with fourth and fifth generation polyamidoamine dendrimers.

Key words : Oxidation of ethanol, Ruthenium oxide, Impedance spectroscopy, Nanosized electrode, Nickel oxide

1. Introduction

RuO_2-coated electrodes have been utilized as anodes in chloroalkali industries due to their excellent corrosion resistance and electrocatalytic activity.[1-4] RuO_2-coated Ti electrodes have also been used as electrodes for both hydrogen[1] and oxygen[5-6] evolution. The loss of anode activity may be related to the loss of RuO_2 from the coating that may lead to the formation of a poorly conducting oxide or an insulating TiO_2 layer on the thermally prepared RuO_2-coated Ti electrode.

Thermally prepared RuO_2-modified Ni electrode was used as a cathode for hydrogen evolution reaction.[2-4] Iwakura *et al.*[2,3] concluded that this electrode diplays enhanced electrocatalytic activity of the cathode due to the increase in active sites or the content of RuO_2 particles. Also, studies on the surface adsorbed species were investigated by the ac impedance spectroscopy on the modified electrodes.[7-10]

In our previous work, we demonstrated effects of the Ni substrate for oxidation of ethanol on the RuO_2-modified Ni electrode surface.[11] Redox couples of RuO_2, *i.e.*, ruthenate (Ru(VI))/perruthenate (Ru(VII)), and nickel, *i.e.*, nickel hydroxide ($Ni(OH)_2$)/nickel oxyhydroxide (NiOOH), were shown to be involved in the electrooxidation of ethanol at the thermally prepared RuO_2-modified Ni electrodes in alkaline media. Therefore, the impedance responses of oxidation of the electrode itself, as well as ethanol, are important in understanding the mechanism of a direct ethanol fuel cell (DEFC) utilizing the RuO_2-modified nickel electrode. In this work, we carried out a study of the impedance responses for oxidation of ethanol. The reactions of ethanol oxidation as well as the passivation of the electrode were modeled using equivalent circuits, and interpretations were made with the parameters used to fit the observed electrochemical impedance spectroscopic (EIS) behavior.

2. Experimental

A nickel wire (Johnson Matthey, 99.99%, 1.0 mm dia.) was used to prepare RuO_2-modified nickel as a working electrode. Preparation of RuO_2-modified nickel electrode was similar to that described in elsewhere.[11] Doubly distilled water and reagent grade chemicals were used for the preparation of the solutions. Each solution was purged with nitrogen for 10 min before measurements. The geometric area of the electrode was 0.17 cm^2. Cyclic voltammograms were recorded using an EG&G model 283 potentiostat/galvanostat, which was controlled by 270 M electrochemistry software. An Ag/AgCl (in saturated KCl) electrode was used as the reference and a platinum wire spiral was used as a counter electrode. The EIS experiments employed an EG&G model 283 potentiostat/galvanostat in conjunction with a Solartron SI 1255 HF frequency response analyzer, which was driven by EG&G M398 electrochemical impedance software. The ac amplitude was 5 mV peak-to-peak for all frequency ranges. The measurements were made at a rate of ten points per decade between 100 kHz and 0.01 Hz at a stationary electrode. Impedance spectra were measured at a stabilized electrode cycled in 1 M KOH until a steady-state cyclic voltammogram was obtained.

†E-mail: smpark@postech.edu

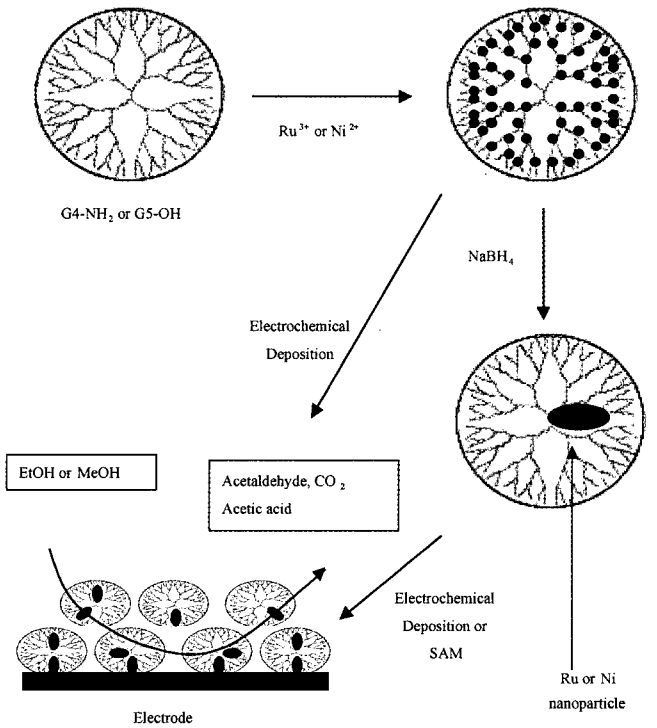

Fig. 1. Schematic diagram for the preparation of nanoparticles by electrochemical deposition and/or chemical reduction of Ru, Ni, or Ru-Ni ions complexed within G4(NH_2) and/or G5(OH) PAMAM dendrimers.

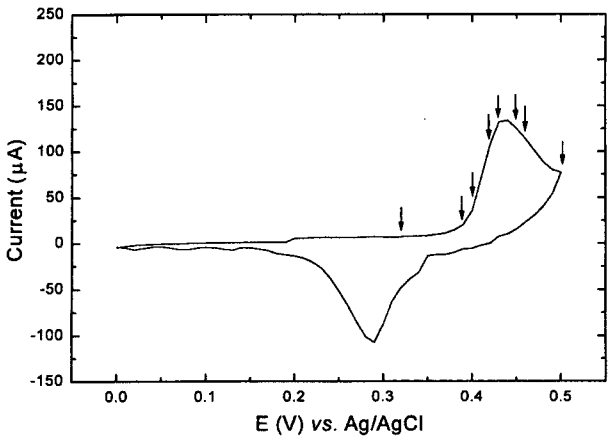

Fig. 2. Cyclic voltammogram of a RuO_2-modified nickel electrode (0.17 cm^2) in 1 M KOH at 10 mV/s. Impedance measurements were made at potentials marked.

For an analysis of impedance data, a software program, "Equivalent Circuit", provided through EG&G by the University of Twente[12] was used. The program simulated a variety of electrical circuits to numerically fit the measured impedance data. Details of circuit analysis using this program and their application to the interpretation of electrode/electrolyte interfaces have been described elsewhere.[12-15]

Ru, Ni, and Ru-Ni binary nanoparticles were prepared by first preloading an amine-terminated poly(amidoamine) (PAMAM) dendrimers (G4(NH_2), where G4 represents the 4th generation), and/or hydroxyl-terminated PAMAM (G5-OH) dendrimers with these metal ions, followed by electrochemical deposition and/or chemical reduction of these composites (Fig. 1). The Ru-Ni binary nanoparticles are prepared by a potentiostatic method in a mixed solution containing G4(NH_2) dendrimers with Ru(III) ions and Ni(0) ions loaded into G5(OH) dendrimer pre-reduced with 10^{-3} M $NaBH_4$.

3. Results and Discussion

A steady-state cyclic voltammogram acquired for the RuO_2-modified Ni electrode in 1 M KOH at 10 mV/s is shown in Fig. 2. The anodic and cathodic peaks appear at 0.43 and 0.30 V *vs.* Ag/AgCl, respectively.

The electrochemical impedance spectra for oxidation of the RuO_2-modified Ni electrode in 1 M KOH were recorded between 0.32 and 0.50 V *vs.* Ag/AgCl at the potentials marked on the cyclic voltammogram shown in Fig. 2. The potential was stepped anodically and impedance spectra were recorded from 0.32 V to a point of interest. The equivalent circuits were derived from the simulation of the experimental data. All the parameters obtained from the simulation are listed in Table 1.

A typical complex impedance spectrum recorded at 0.32 V is shown in Fig. 3. In all potential ranges, the value of R_S (solution resistance) was 3.9±0.2 Ω. The equivalent circuit

Table 1. Parameters Used for Equivalent Circuits for Electrode Oxidation

E_{app} (V)	R_1 (Ω)[b]	R_2 (Ω)[b]	R_3 (Ω)[b]	Q_1		Q_2		Q_3		Q_4		Q_5		Q_6		Q_7		τ_{high} (s)[c]	τ_{low} (s)[d]	χ^2 (×10^{-4})[e]
				Y_Q×10^{-5}	n	Y_Q×10^{-4}	n	Y_Q×10^{-3}	n	Y_Q×10^{-4}	n	Y_Q×10^{-3}	n	Y_Q×10^{-7}	n	Y_Q×10^{-4}	n			
0.32	1.37	954.4	–	83.7	0.41	15.5	0.74	1.3	0.83	3.5	0.88	–	–	4.0	-1.00	6.6	0.80	0.1949	–	0.41
0.39	4.15	156.1	–	21.5	0.81	–	–	1.4	0.51	2.2	0.77	–	–	63.9	-1.00	30.2	0.81	0.0412	–	3.35
0.40	1.23	40.3	–	6.2	0.93	–	–	2.8	0.49	7.9	0.69	–	–	40.2	-1.00	18.4	0.77	0.0109	–	1.88
0.42	–	11.6	1872.3	–	–	–	–	–	–	21.2	0.65	5.1	0.91	33.1	-1.00	17.1	0.73	0.0020	14.05	1.97
0.43	–	17.2	13750.0	–	–	–	–	7.1	0.49	15.5	0.65	1.5	0.83	–	–	–	–	0.0038	38.54	3.24
0.45	–	16.5	11190.0	–	–	–	–	22.6	0.43	24.0	0.62	1.3	0.81	–	–	–	–	0.0059	34.93	14.60
0.46	–	5.1	10222.0	–	–	–	–	4.2	0.45	7.8	0.72	1.7	0.89	–	–	–	–	0.0039	41.86	37.10
0.50	–	2.1	1974.6	–	–	–	–	14.6	0.20	29.4	0.62	1.4	0.84	–	–	–	–	0.0040	5.87	11.70

[a] R_S values are not listed as they are almost constant at 3.9±0.2Ω for measurements made between 0.32 and 0.50 V.
[b] R_P-values were taken as R_1+R_2 or R_3.
[c] τ_{high} is a time constant at high frequency region.
[d] τ_{low} is a time constant at low frequency region.
[e] Chi square values for the equivalent circuits fitting.

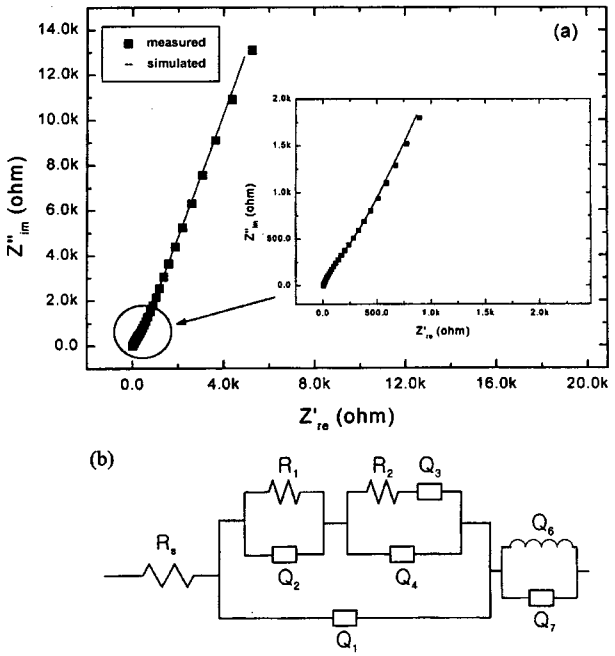

Fig. 3. (a) Complex impedance responses for oxidation of the RuO_2-modified nickel electrode at 0.32 V in 1 M KOH; (b) an equivalent circuit used in the CNLLS fitting procedure.

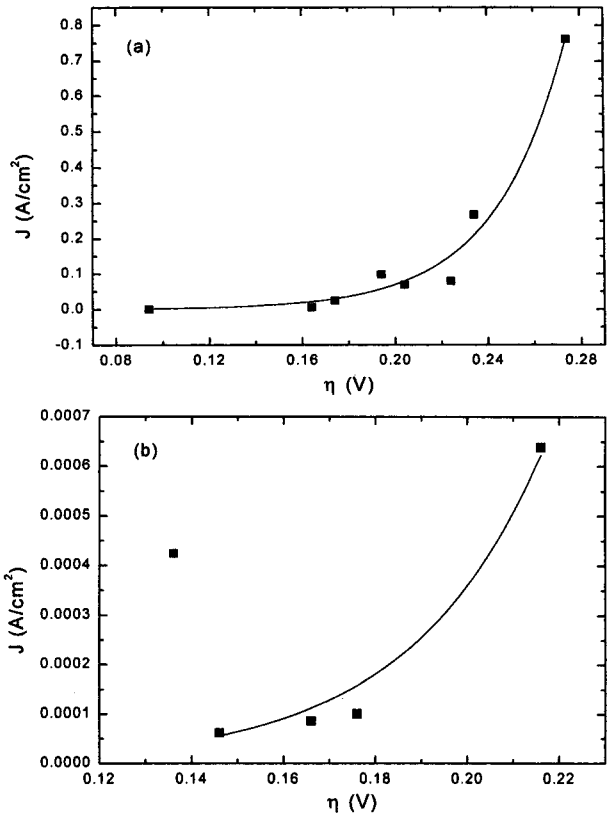

Fig. 4. (a) Current density calculated from $R_1 + R_2$ *vs.* overpotential in 1 M KOH. The line drawn is from nonlinear least squares (NLS) fitting using Butler-Volmer equation for the data between 0.32 and 0.50 V; (b) current density *vs.* overpotential for R_3 in 1 M KOH with the NLS line drawn for the data between 0.42 and 0.50 V.

having two parallel RC networks connected in parallel with Q_1 as shown in Fig. 3b represents two faradaic reactions taking place at this potential with charge-transfer resistances of R_1 and R_2. The use of constant phase elements (CPEs) is proper for the RuO_2-modified Ni electrode instead of double-layer capacitance, considering the surface roughness of the porous electrode and the formation of various oxides. CPEs Q_2 and Q_4 appear to be related to the pseudo-capacitance with *n*-values close to 1.0 (0.74 and 0.88) due to the adsorption, which is not affected by the porosity of the passive films in the inner pores in a high frequency range, while Q_3 is a pseudo-capacitor developed in the outer pores of the films. A Warburg component with an *n* value close to 0.5 (the element with a symbol Q_3 in the circuit) is observed in most of the potential ranges except at 0.32 V, indicating that the kinetics of the oxidation process is limited by the diffusion of the oxidation products into the inner pores of the passive film. CPEs, Q_6 and Q_7, in Table 1 represent the inductor and pseudo-capacitor in the low frequency range with *n* values of -1.00 and 0.80, respectively. The low frequency inductive response may indicate that the rapid transformation of ruthenate to perruthenate in the potential range, where nickel oxidation does not occur, is impeded at the electrode/electrolyte interface by the inductive current of the nickel electrode itself flowing in the opposite direction. The low frequency capacitive response may be related to the adsorbed intermediate species generated during the oxidation process. The reaction taking place at 0.32 V is most likely the oxidation reaction of ruthenate to perruthenate.

Current densities were calculated using Ohm's law from the overpotentials applied and R_P values. A plot of current density *vs.* overpotential shown in Fig. 4 was obtained using the data listed in Table 1. The current density *vs.* overpotential in the medium frequency region shown in Fig. 4a should be due to oxidation of ruthenate to perruthenate, whereas the result in the low frequency region shown in Fig. 4b should be due to oxidation of nickel hydroxide to nickel oxyhydroxide on the passive film. The nonlinear least squares regression was used to evaluate kinetic parameters for the oxidation of ruthenate using the equation $i=i_O(\exp(-\alpha n f\eta)-\exp((1-\alpha)nf\eta))$, where i_O is the exchange current, α is the transfer coefficient, f is F/RT, and η is the overpotential. From the regression, the exchange current density, i_O, for the rate limiting one-electron charge-transfer reaction was calculated to be 1.1×10^{-4} A/cm^2 at the equilibrium potential, 0.226 V *vs.* Ag/AgCl[16] with a transfer coefficient, α, of 0.17. From the regression between 0.43 and 0.50 V shown in Fig. 4b, the kinetic parameters for the oxidation of nickel hydroxide at the RuO_2-modified nickel electrode can be calculated as having an i_O value of 3.8×10^{-7} A/cm^2 at the equilibrium potential of 0.284 V *vs.* Ag/AgCl,[17] with the α value of 0.12. These values may be compared with i_O and α values of 7.0×10^{-5} A/cm^2 and 0.25, respectively, obtained by our previous work at the nickel electrode.[18] The kinetic parameters of the nickel at the RuO_2-modified nickel electrode may be small due to the different electrode conditions and the area of the active site.

A typical steady-state cyclic voltammogram obtained for oxidation of 0.20 M ethanol at the RuO_2-modified nickel

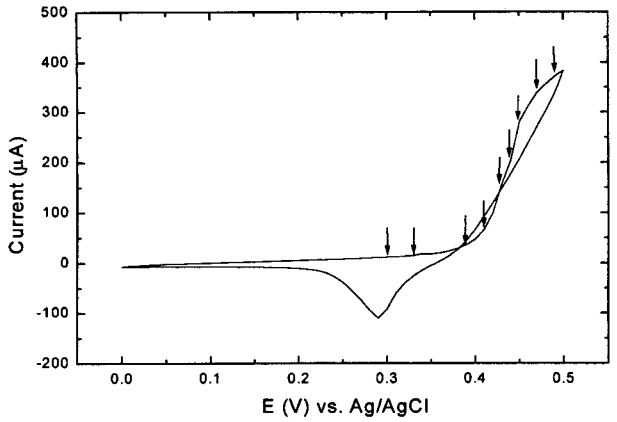

Fig. 5. Cyclic voltammogram for oxidation of 0.20 M ethanol at a RuO_2-modified nickel electrode (0.17 cm^2) in 1 M KOH at 10 mV/s. Impedance measurements were made at potentials marked.

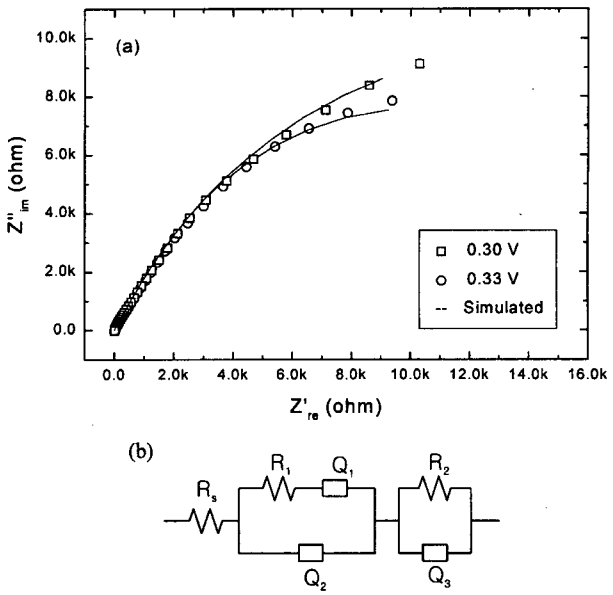

Fig. 6. (a) Complex impedance responses for oxidation of ethanol at RuO_2-modified nickel electrode at 0.30 and 0.33 V in 1 M KOH containing 0.20 M ethanol; and (b) An equivalent circuit used in the CNLLS fitting procedure.

electrode in 1 M KOH is shown in Fig. 5. The electrode appears passivated as evidenced by the nucleation loop observed around 0.40 V, although the passivation is not as severe as at the platinum electrode.[19] The electrochemical impedance spectra for oxidation of 0.20 M ethanol in 1 M KOH were recorded between 0.30 and 0.49 V *vs.* Ag/AgCl at the potentials marked on the cyclic voltammogram. All the parameters obtained from the complex nonlinear least squares (CNLS) fitting are listed in Table 2.

The complex impedance spectra recorded at 0.30 and 0.33 V are shown in Fig. 6. In all potential ranges measured, the solution resistance, R_S, was 4.8±0.6 Ω. The introduction of ethanol raised the R_S value by about 1 Ω. The high frequency response at 0.30 V is essentially the same as that at 0.32 V in 1 M KOH. The resistance R_2 may be representing that for adsorption of reactant corresponding to a CPE (Q_3) with an n value of 0.75. The low frequency spectrum at 0.33 V may be a response caused by ruthenate oxidation limited by mass-transfer having a Warburg response (Q_1).

Plots of current density *vs.* overpotential shown in Fig. 7 were obtained using the data listed in Table 2. The current density *vs.* overpotential for R_1 shown in Fig. 7a should be due to oxidation of ruthenate to perruthenate, whereas the result in the low frequency region shown in Fig. 7b should be due to oxidation of ethanol on the oxide films. From the nonlinear regression of the data between 0.33 and 0.45 V, the exchange current density, i_O, for the rate limiting one-electron charge-transfer reaction was calculated to be 5.1×10^{-4} A/cm^2 at the equilibrium potential of 0.226 V *vs.* Ag/AgCl[16] with α of 0.34. From the regression between 0.30 and 0.49 V the kinetic parameters for ethanol oxidation at the RuO_2-modified nickel electrode can be calculated as having an i_O value of 2.7×10^{-10} A/cm^2 at the equilibrium potential of -0.967 V *vs.* Ag/AgCl[19-21] with an α value of 0.92. These values present that the RuO_2-modified nickel electrode improves ethanol oxidation comparing with i_O and α values of 2.7×10^{-19} A/cm^2 and 0.82, respectively, obtained at the nickel electrode.[18] Also, the α-value may be compared with that obtained by Shieh

Table 2. Parameters used for equivalent circuits for oxidation of 0.20 M ethanol in 1 M KOH

$E_{applied}$ (V)	R_1 (Ω)[b]	R_2 (Ω)[c]	R_3 (Ω)[c]	Q_1		Q_2		Q_3		Q_4		τ_{high} (s)[d]	τ_{low} (s)[e]	χ^2 ($\times10^{-4}$)[f]
				$Y_Q\times10^{-4}$	n	$Y_Q\times10^{-4}$	n	$Y_Q\times10^{-4}$	n	$Y_Q\times10^{-4}$	n			
0.30	1.29	28461.0	–	6.14	1.00	46.95	0.27	4.96	0.75	–	–	0.0182	130.19	8.93
0.33	755.98	16478.0	–	23.35	0.40	5.59	0.75	7.32	0.87	–	–	0.1502	87.96	4.40
0.39	44.53	635.6	4226.1	–	–	9.00	0.95	9.10	0.70	12.45	0.87	0.0245	30.50	1.32
0.41	8.10	152.7	931.1	–	–	10.21	0.87	20.97	0.62	18.43	0.79	0.0081	1.45	0.30
0.43	10.98	347.8	383.7	–	–	14.54	0.77	22.51	0.62	28.82	0.89	0.0045	0.95	0.33
0.44	9.09	277.9	306.9	–	–	23.55	0.71	30.72	0.86	27.00	0.62	0.0017	0.68	0.45
0.45	8.56	279.7	322.1	–	–	27.19	0.69	28.84	0.63	28.03	0.84	0.0016	0.54	4.24
0.47	14.50	85.0	553.6	–	–	31.59	0.62	44.43	0.68	18.24	0.80	0.0020	0.71	0.60
0.49	293.76	22.0	461.7	–	–	19.24	0.75	36.31	0.60	29.86	0.92	0.0061	0.61	0.66

[a] R_S values are not listed as they are almost constant at 4.8±0.6Ω for measurements made between 0.30 and 0.49 V.
[b] R_P was taken as R_1 at all applied potentials.
[c] R_P was taken as R_2+R_3 at all applied potential.
[d] τ_{high} is a time constant in the high frequency region.
[e] τ_{low} is a time constant in the low frequency region.
[f] Chi square values for the equivalent circuits fitting.

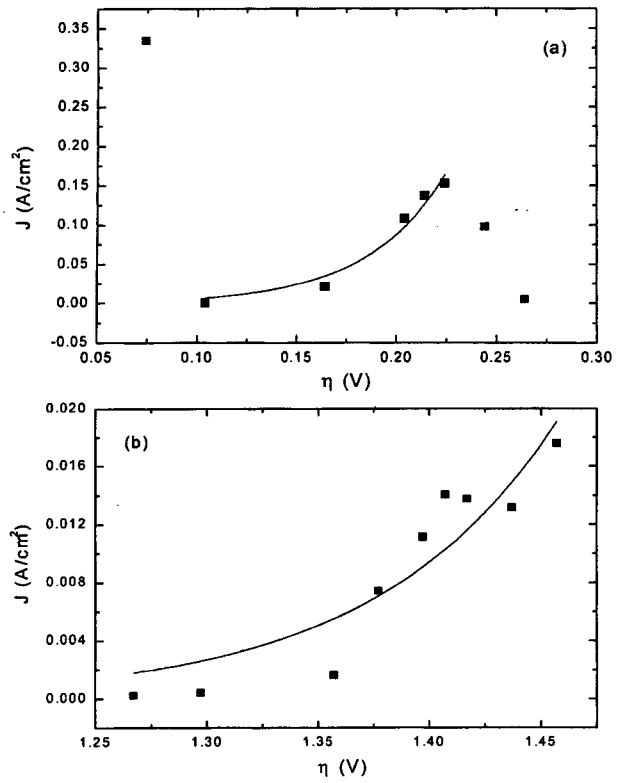

Fig. 7. (a) The current density *vs.* overpotential for R_1 for oxidation of 0.20 M ethanol in 1 M KOH. The line drawn is from the nonlinear least squares fitting for the data between 0.33 and 0.45 V; (b) Current density *vs.* overpotential for R_2. The nonlinear least squares curve fitting is drawn for the data obtained between 0.30 and 0.49 V.

and Hwang (0.75) for ethanol oxidation at the thermally prepared RuO_2 on titanium in 1 M KOH.[22] Their value of 0.75 was derived from rotating-disk electrode and polarization studies at the RuO_2/Ti electrode.

Finally, the results obtained at the nanosized electrocatalysts are described. The proton diffusion coefficient at the bulk nickel hydroxide electrode was reported to be 10^{-11} cm^2/s for irreversible reaction from cyclic voltammetric studies[23] and impedance measurements.[18] The proton diffusion coefficient obtained at Ru/G4(NH_2)-Ni/G5(OH) nanoparticles is about two orders of magnitude larger, at about ~10^{-9} cm^2/s. The exchange current density at 1.9×10^{-7} A/cm^2 observed at templated Ru/Ni electrode indicates that oxidaton of the templated nanoparticle electrode is very fast due to the surface reaction. Dendrimer templated metal nanoparticles show improved electrochemical properties due to their well segregated aggregates between particles, resulting in increases of surface areas.

4. Conclusion

The exchange current for the ruthenate/perruthenate transition was estimated to be 1.1×10^{-4} A/cm^2 with an α-value of 0.17, while it is 3.8×10^{-7} A/cm^2 with an α-value of 0.12 for the nickel hydroxide/nickel oxyhydroxide transition. The redox couples of the Ru(VI)/Ru(VII) and $Ni(OH)_2$/NiOOH pairs at the RuO_2-modified nickel electrode were shown to act as effective electron transfer mediators for ethanol oxidation. The exchange current for the ruthenate/perruthenate transition with ethanol present was estimated to be 5.1×10^{-4} A/cm^2 with an α-value of 0.34 and the exchange current for the ethanol oxidation was estimated to be 2.7×10^{-10} A/cm^2, with an α-value of 0.92.

The catalytic activity for ethanol oxidation was improved by about four orders of magnitude as the exchange current was observed to be 1.9×10^{-7} A/cm^2, when RuO_2-modified nickel nanosized particle electrode was used. The performance was much improved for single component electrodes when the metal electrodes of nanosized particles were used. The catalysts of nanosized particles offer promises for many energy conversion devices.

Acknowledgment

This work was partially supported by a grant from the Ministry of Education through the School of Environmental Engineering at Pohang University of Science and Technology and the R&D Management Center for Energy and Resources.

References

1. L. L. Chen, D. Guay and A. Lasia, *J. Electrochem. Soc.*, **143**, 3576 (1996).
2. C. Iwakura, N. Furukawa and M. Tanaka, *Electrochim. Acta*, **37**, 757 (1992).
3. C. Iwakura, M. Tanaka, S. Nakamatsu, H. Inoue, M. Matsuoka and N. Furukawa, *Electrochim. Acta*, **40**, 977 (1995).
4. N. Spararu, J. G. Le helloco and R. Durand, *J. Appl. Electrochem.*, **26**, 397 (1996).
5. L. D. Burke and M. McCarthy, *Electrochim. Acta*, **29**, 211 (1984).
6. L. D. Burke, O. J. Murphy, J. F. ONeill and S. Venkatesan, *J. Chem. Soc. Faraday Trans. 1*, **73**, 1659 (1977).
7. Y. Choquette, L. Brossard, A. Lasia and H. Menard, *J. Electrochem. Soc.*, **137**, 1723 (1990).
8. P. Ekdunge, K. Juttner, G. Kreysa, T. Kessler, M. Ebert and W. J. Lorenz, *J. Electrochem. Soc.*, **138**, 2660 (1991).
9. P. Gu, L. Bai, L. Gao, R. Brousseau and B. E. Conway, *Electrochim. Acta*, **37**, 2145 (1992).
10. M. Okido, J. K. Depo and G. A. Capuano, *J. Electrochem. Soc.*, **140**, 127 (1993).
11. J.-W. Kim and S.-M. Park, *J. Electrochem. Soc.*, **146**, 1075 (1999).
12. B. A. Boukamp, *Equivalent Circuit Users Manual*, 2nd ed., University of Twente, Enschede, the Netherlands (1989).
13. B. J. Johnson and S.-M. Park, *J. Electrochem. Soc.*, **143**, 1269 (1996).
14. M. Cai and S.-M. Park, *J. Electrochem. Soc.*, **143**, 3859 (1996).
15. D. K. Cha and S.-M. Park, *J. Electrochem. Soc.*, **144**, 2573 (1997).
16. E. J. M. OSullivan and J. R. White, *J. Electrochem. Soc.*, **136**, 2576 (1989).
17. A. J. Bard, *Encyclopedia of Electrochemistry of the Elements*, Vol III, Marcel Dekker, Inc., New York, 1975.
18. J.-W. Kim and S.-M. Park, submitted for publication (1999).
19. S.-M. Park, N. C. Chen, and N. Doddapaneni, *J. Electrochem. Soc.*, **142**, 40 (1995).
20. L. W. H. Leung, S. C. Chang and M. J. Weaver, *J. Electroanal. Chem.*, **266**, 317 (1989).
21. P. Gao, S. C. Chang, Z. Zhou and M. J. Weaver, *J. Electroanal. Chem*, **272**, 161 (1989).
22. D. T. Shieh and B. J. Hwang, *J. Electrochem. Soc.*, **142**, 816 (1995).
23. C. Zhang and S.-M. Park, *J. Electrochem. Soc.*, **134**, 2966 (1987).